

## Dynamic redistribution of calmodulin in HeLa cells during cell division as revealed by a GFP-calmodulin fusion protein technique

Chao-Jun Li<sup>1,\*</sup>, Roger Heim<sup>2</sup>, Pin Lu<sup>1</sup>, Yongmei Pu<sup>1</sup>, Roger Y. Tsien<sup>2</sup> and Donald C. Chang<sup>1,†</sup>

<sup>1</sup>Department of Biology, Hong Kong University of Science and Technology, Clear Water Bay, Hong Kong

<sup>2</sup>Howard Hughes Medical Institute, University of California at San Diego, La Jolla, CA 92093-0647, USA

\*On leave from Nanjing Normal University, Nanjing 210097, China

†Author for correspondence (e-mail: bochang@ust.hk)

Accepted 1 March; published on WWW 22 April 1999

### SUMMARY

It has been suggested by many studies that  $\text{Ca}^{2+}$  signaling plays an important role in regulating key steps in cell division. In order to study the down stream components of calcium signaling, we have fused the gene of calmodulin (CaM) with that of green fluorescent protein (GFP) and expressed it in HeLa cells. The GFP-CaM protein was found to have similar biochemical properties as the wild-type CaM, and its distribution was also similar to that of the endogenous CaM. Using this GFP-tagged CaM as a probe, we have conducted a detailed examination of the spatial- and temporal-dependent redistribution of calmodulin in living mammalian cells during cell division. Our major findings are: (1) high density of CaM was found to distribute in two sub-cellular locations during mitosis; one fraction was concentrated in the spindle poles, while the other was concentrated in the sub-membrane region

around the cell. (2) The sub-membrane fraction of CaM became aggregated at the equatorial region where the cleavage furrow was about to form. The timing of this localized aggregation of CaM was closely associated with the onset of cytokinesis. (3) Using a TA-CaM probe, we found that the sub-membrane fraction of CaM near the cleavage furrow was selectively activated during cell division. (4) When we injected a CaM-specific inhibitory peptide into early anaphase cells, cytokinesis was either blocked or severely delayed. These findings suggest that, in addition to  $\text{Ca}^{2+}$  ion, CaM may represent a second signal that can also play an active role in determining the positioning and timing of the cleavage furrow formation.

Key words: Cytokinesis, Cell division, Calmodulin, Calcium signaling, GFP

### INTRODUCTION

Cell division is a precisely regulated process that is believed to be controlled by a number of different cellular signals. Besides the well-known cyclin-dependent kinase system, second messengers like  $\text{Ca}^{2+}$  and cyclic AMP are also thought to be involved (for reviews, see Berridge, 1995; Hepler, 1994; Means, 1994; Whitaker, 1995). In fact, findings from recent studies have shown that an elevation of intracellular free calcium ions is correlated with several important mitotic events, including nuclear envelope breakdown and metaphase-anaphase transition (Poenie et al., 1986; Ratan et al., 1988; Tombes and Borisy, 1989; Kao et al., 1990; Li et al., 1994; Muto et al., 1996; Bos-Mikich et al., 1997). Using the zebrafish embryo as a model system, we have also demonstrated that a localized elevation of  $\text{Ca}^{2+}$  level is closely associated with the onset of cytokinesis (Meng and Chang, 1994; Chang and Meng, 1995). These findings strongly suggest that  $\text{Ca}^{2+}$  signal plays an important role in regulating cell division.

A natural question that follows is whether the down stream molecules of the  $\text{Ca}^{2+}$  signaling pathway may also play an active role in such a regulation mechanism. The major

intracellular calcium receptor is calmodulin (CaM). The binding of  $\text{Ca}^{2+}$  to CaM enables it to activate various target enzymes and thereby regulate many physiological processes (for reviews, see Wang et al., 1985; Means et al., 1991; Vogel, 1994; Finn and Forsen, 1995; Niki et al., 1996; Rhoads and Friedberg, 1997). The involvement of CaM in cell cycle regulation has been suggested in several earlier studies (Rasmussen et al., 1992; Lu and Means, 1993; Takuwa et al., 1995; Török et al., 1998). One key area that we wanted to examine in detail in this investigation was the dynamic redistribution of CaM during the initiation of cytokinesis. Our main question was whether the distribution of CaM may play a role in determining the timing and positioning of the cleavage furrow formation. This question is related to a dilemma currently found in the literature. In large cells such as the embryonic cells of zebrafish or *Xenopus*, there is clear evidence that a localized elevation of  $\text{Ca}^{2+}$  is spatially and temporally associated with the onset of cytokinesis (Chang and Meng, 1995; Muto et al., 1996; Webb et al., 1997). Similar evidence, however, has been lacking in the smaller size mammalian cells. In fact, it has been suggested that a gradual rise of  $\text{Ca}^{2+}$  concentration, rather than a localized  $\text{Ca}^{2+}$  transient, was

required for the progression of cell division in mammalian cells (Tombes and Borisy, 1989). Then, what is the signal that determines the timing and positioning of the cleavage furrow formation? One possible answer is that a population of the  $\text{Ca}^{2+}$  receptor (calmodulin) may be specially localized at the cell equator in mammalian cells; its activation by a broadly rising  $\text{Ca}^{2+}$  signal will then trigger the formation of the cleavage furrow at the proper place.

We would like to examine this hypothesis by imaging the CaM distribution in living cells over the entire cell division process using a GFP-labeling technique. GFP (green fluorescent protein) is a natural fluorescent protein discovered

the poration medium (260 mM mannitol, 5 mM sodium phosphate, 10 mM potassium phosphate, 1 mM  $\text{MgCl}_2$ , 10 mM Hepes, 4 mM ATP, 0.1 mM BAPTA, pH 7.3) in a concentration of  $4 \times 10^5$  cells per ml. 100  $\mu\text{l}$  of the cell suspension was mixed with 5  $\mu\text{g}$  of plasmid DNA and placed into the electroporation chamber. The cells were then electroporated using a procedure previously described (Chang et al., 1991; Chang, 1997). After electroporation, cells were incubated in a recovery medium (culture medium supplemented with 0.5 mM BAPTA and 2 mM  $\text{MgCl}_2$ ) for 30 minutes and then returned to normal culturing. Cells were usually cultured for at least 24 hours for expressing the introduced gene.

#### **Immunofluorescence staining**

The immunostaining procedure was essentially that of Harlow and

sections taken at different focus planes (Z-series measurement). Results of these measurements were then displayed either as projected images or 3-D images.

### Living cell observation

To study the redistribution of GFP-CaM in living cells, fluorescent signals of mitotic cells expressing the fusion gene were examined continuously for several hours using a digital video imaging system. The transfected cells were cultured on a 25 mm diameter round coverslip, which was placed in a thermally regulated chamber (Medical System Corp., Greenvale, NY) mounted on the stage of a Zeiss Axiovert 35 inverted microscope (Carl Zeiss, Oberkochen, Germany). The fluorescent image of GFP was observed using a FITC filter set. The excitation light was controlled using a Lambda-10 filter wheel shutter (Sutter Instrument Company, Novato, CA). The images were recorded using either a MicroMax digital camera with cooling system (Princeton Instrument Ltd, Trenton, NJ) or a DEI-470 CCD video camera system (Optromics Engineering, Goleta, CA). The image recording, analysis, as well as shutter control, were done by a computer using MetaMorph software (Universal Image Corporation, West Chester, PA). In order to minimize photo damage to cells, images (using 0.5 to 2 seconds exposure) were recorded only once every minute; excitation light was reduced using neutral density filters and was blocked between image recording. Also, an oxygen scavenger called 'oxyrase' (obtained from Oxyrase, Inc., Ashland, OH) was added to the cell culture medium (0.3 units/ml) to protect cells from photodynamic damage (Waterman-Storer et al., 1993).

### TA-CaM measurement

To image the pattern of CaM activation during cell division, we injected CaM labeled with 2-chloro-( $\epsilon$ -amino-Lys<sub>75</sub>)-[6-(4-*N,N*-diethylaminophenyl)-1,3,5-triazin-4-yl] (TA-calmodulin) into the M-phase HeLa cells. This probe was prepared by Dr Weiming Dai and Mingjie Zhang (Hong Kong University of Science and Technology) following the procedures described by Török and Trentham (1994). It was shown that the fluorescent intensity of the TA-CaM molecule increased 9-fold when it was activated by Ca<sup>2+</sup> and bound to a target protein (Török and Trentham, 1994; Török and Whitaker, 1994). TA-CaM was usually injected at the pro-metaphase. Its fluorescent image was then recorded periodically in an interval of 20 seconds using an Axiovert microscope (Zeiss) and a cooled CCD camera (Princeton Instrument).

### Microinjection of inhibitors

The activity of CaM within the living cells can be inhibited by injecting CaM-specific inhibitory peptides into the cells. Two peptides were used in this study. The first one, called 'Trp peptide' (Ac-RRKWQKTGHAVRAIGRL-NH<sub>2</sub>), resembled the CaM-binding region of MLCK (myosin light chain kinase) and had a very high affinity with CaM (dissociation constant  $K_d = 0.006 \pm 0.002$  nM) (Török and Trentham, 1994). The second one, called 'Tyr peptide' (Ac-RRKYQKTGHAVRAIGRL-NH<sub>2</sub>), differed from the Trp peptide

by one amino acid and was shown to have a much lower affinity to CaM ( $K_d = 3.6 \pm 0.4$  nM) (Török and Trentham, 1994). It was used here as a control. These peptides were obtained from Tana Laboratories (Houston, TX) and had been purified by HPLC.

The microinjection was performed using an Eppendorf microinjection system, which consisted of a Transjector (Eppendorf 5246) and a Micromanipulator (Eppendorf 5171) that were mounted on a Zeiss Axiovert 100 microscope. Peptide (5 mM) mixed with FITC-conjugated 10 kDa dextran (150 mM) was filled into an Eppendorf Femtotip and injected into anaphase cells before cytokinesis. The volume of the injection solution was typically less than 5% of the cell volume.

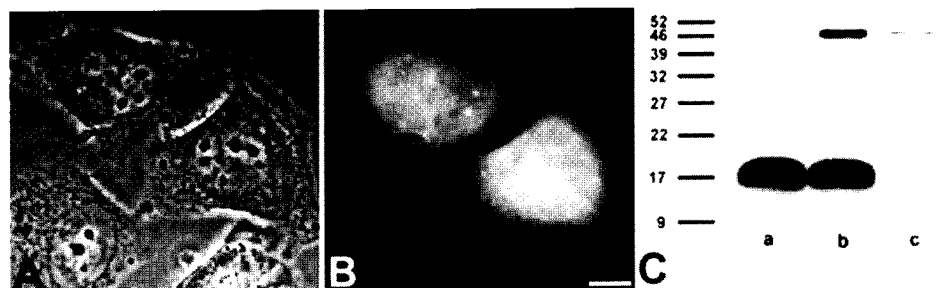
## RESULTS

### Expression of GFP-CaM in HeLa cells

After the GFP-CaM fusion gene was introduced into HeLa cells by electroporation, many cells were found to express this gene and produce the fluorescent protein. The presence of this protein can be observed easily using an epi-fluorescence microscope equipped with a FITC filter set. The GFP-CaM fusion protein was detected as early as 10 hours after transfection. The expression reached an optimal level about one day of culturing. The fluorescence of the fusion protein was relatively stable; it could be detected for at least three days after the GFP-CaM fusion gene had been expressed. In most experiments, approximately 20% of the targeted cells were found to express the fusion gene. A typical result is shown in Fig. 1. The phase image of the transfected cells that have been cultured for one day is shown in A. The fluorescent image of the same cells is shown in B. It can be seen that two cells had expressed the GFP-CaM fusion gene and gave a bright fluorescent image.

To verify that the fluorescent signal was indeed generated by the gene product of the GFP-CaM fusion gene, we conducted a western blot experiment to examine the existence of such a protein. The results are shown in Fig. 1C. In lane a, protein extract from the control HeLa cells (i.e. non-transfected cells) was stained with antibody against CaM. Only one major band was observed; its estimated molecular mass (17 kDa) indicated that it is the endogenous CaM. In lane b, protein extract from the HeLa cells transfected with the fusion gene was stained with anti-CaM. Two bands were observed. The darker band with the same molecular mass as that in lane a undoubtedly represented the endogenous CaM. The lighter new band had an approximate molecular mass of 45 kDa, which was close to the expected molecular mass of the GFP-CaM fusion protein. Indeed, this band was also stained positively with antibody

**Fig. 1.** Expression of the GFP-CaM fusion gene in HeLa cells. The fusion gene was introduced into cells by electroporation. After one day of culturing, some cells were found to produce the fluorescent gene product. (A and B) Samples of these cells in phase optics and fluorescent image, respectively. Bar, 10  $\mu$ m. (C) The results of western blots assaying the expression of the GFP-CaM fusion gene. Lane a was from lysate of control cells, while lanes b and c were from lysate of GFP-CaM transfected cells. Lanes a and b were stained using anti-CaM antibody, while lane c was stained using anti-GFP antibody.



against GFP (lane c of Fig. 1C), indicating that it does represent the GFP-CaM fusion protein. By comparing the relative intensity of the two bands in lane b of Fig. 1C (and taking into consideration that only 20% of the transfected cells had expressed the fusion gene), we estimate that the average amount of GFP-CaM fusion protein produced in an expressed cell was about 42% of that of the endogenous CaM. Thus, it was not surprising that the expression of the GFP-CaM fusion gene apparently did not interfere with the normal cellular functions (including cell division) of the transfected cells.

### The function of the GFP-tagged calmodulin protein is similar to that of the wild-type calmodulin

In order to use the GFP-CaM fusion protein as a probe to study the distribution of the endogenous CaM in living cells, we want to make sure that the properties of this GFP-tagged CaM protein are basically similar to those of the untagged protein. Specifically, we want to examine if the GFP-tagged CaM can still bind  $\text{Ca}^{2+}$  ions effectively, and, such a binding can induce the CaM to activate its target enzyme. It is known that CaM and other high-affinity  $\text{Ca}^{2+}$ -binding proteins show a significant  $\text{Ca}^{2+}$ -induced shift in electrophoretic mobility, even in presence of SDS (Rhyner et al., 1992). To test whether GFP-CaM can still bind calcium with high affinity and alter its electrophoretic mobility as an effect, acrylamide gel electrophoresis was performed in the presence and absence of  $\text{Ca}^{2+}$  as described by Rhyner et al. (1992). Indeed,  $\text{Ca}^{2+}$  caused the GFP-CaM band to shift from 54 to 48 kDa (Fig. 2A). This downward band shift was very similar to those observed using untagged CaM (Rhyner et al., 1992). To test GFP-CaM for biochemical activity, stimulation of bovine heart phosphodiesterase was measured as a function of GFP-CaM concentration at a fixed  $\text{Ca}^{2+}$  concentration of 0.8 mM. GFP-CaM was able to maximally activate phosphodiesterase threefold, with half maximal activation at 5 nM (Fig. 2B). Also, the  $\text{Ca}^{2+}$  dependence of activation was measured (Fig. 2C). Half maximal stimulation was found to be at 0.1–0.2  $\mu\text{M}$ . These findings are in good agreement with the results reported by Rhyner et al. (1992) for wild-type calmodulin. Thus, the GFP-tagging appears not to significantly affect the functional properties of the CaM molecule.

### The fluorescent image of GFP-CaM reflects the distribution of endogenous CaM in HeLa cells

Since the GFP-CaM fusion protein contained both the GFP protein and the CaM protein, we wanted to know whether the distribution pattern of the GFP-CaM fusion protein reflects mainly the targeting CaM, or GFP. Thus, we have made a detailed comparison between the distribution patterns of GFP-CaM protein and that of pure GFP or endogenous CaM, in both interphase cells and mitotic cells (Fig. 3). In this comparative study, we used a confocal microscope rather than a conventional epi-fluorescence microscope to examine the detailed distribution of the GFP-CaM fusion protein. This is because HeLa cells usually became round-up during cell division. The fluorescence image of the GFP-CaM fusion protein can be recorded clearly only using a confocal microscope.

The distribution pattern of GFP protein was obtained by expressing a vector containing only the GFP gene (i.e. without fusing with CaM) in the HeLa cell. The GFP protein was found

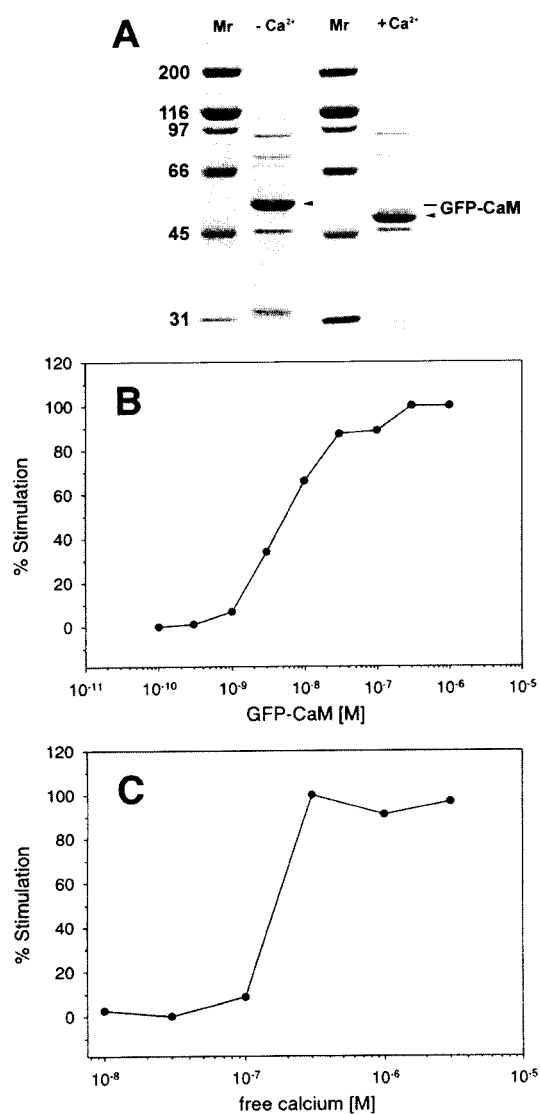


**Fig. 2.** Characterization of recombinant GFP-CaM.

(A) Electrophoretic mobility of GFP-CaM is dependent on binding to  $\text{Ca}^{2+}$ . Two separate SDS polyacrylamide gels were run in the absence of  $\text{Ca}^{2+}$  (left side) and in the presence of 0.1 mM  $\text{Ca}^{2+}$  (right side).  $\text{Ca}^{2+}$  decreased the apparent molecular mass from 54 to 48 kDa (arrowheads). The weaker non-specific bands were not affected by calcium. Protein molecular mass markers from Bio-Rad (Hercules, CA) were run on both gels in the left lane. (B) Activation of 3',5'-cyclic nucleotide phosphodiesterase by GFP-CaM. The relative stimulation of phosphodiesterase as a function of the concentration of GFP-CaM is shown. With the maximal stimulation taken as 100%, half maximal stimulation was achieved at 5 nM GFP-CaM. The free  $\text{Ca}^{2+}$  concentration was 0.8 mM. (C)  $\text{Ca}^{2+}$  dependence of phosphodiesterase stimulation by GFP-CaM. The relative phosphodiesterase stimulation by 1 mM GFP-CaM is plotted as a function of free calcium. The maximal stimulation was set to 100%, and half maximal stimulation was obtained at 0.1–0.2  $\mu\text{M}$  free  $\text{Ca}^{2+}$ .

to be distributed highly evenly in both the interphase cells (Fig. 3A) and the mitotic cell (Fig. 3B), with no visible fine structure. Such a distribution pattern was entirely different from those of the distribution patterns of the GFP-CaM fusion protein (Fig. 3C and D). The distribution patterns of the

endogenous CaM (Fig. 3E and F), in contrast, were very similar to those of the GFP-CaM fusion protein (Fig. 3C and D). This comparison was done by fixing cells that expressed GFP-CaM and then immunostaining them with antibody against CaM. Using a secondary antibody conjugated with rhodamine, the distribution pattern of the endogenous CaM can be visualized in a fluorescence channel different from that of GFP. Thus, the image of the cell at the center of Fig. 3E represents the immunostaining pattern of CaM of the same cell shown in the center of Fig. 3C, where the image represents the fluorescence pattern of the GFP-CaM fusion protein. (Note: the cell at the upper left hand corner of Fig. 3E was a cell that failed to express the GFP-CaM fusion gene.) By comparing Fig. 3C with E, it appears that, at interphase, the distribution pattern of the GFP-CaM fusion protein was very similar to that of the endogenous CaM.

A similar conclusion can also be drawn for mitotic cells. Again, Fig. 3D and F represent the image of GFP-CaM and the immunostaining pattern of anti-calmodulin of a metaphase cell, respectively. By comparing these two figures, it is evident that the distribution pattern of GFP-CaM is similar to the immunostaining pattern of anti-calmodulin. For example, a

high concentration of GFP-CaM was found at the spindle poles of the living mitotic cell (Fig. 3D), while very dense CaM was also found at the poles of the mitotic spindle in the immunostained cell (Fig. 3F). Thus, the fluorescence image of GFP-CaM appears to be in good agreement with the distribution pattern of the endogenous CaM in HeLa cells as indicated by immunostaining.

### A sub-membrane fraction of CaM is found in the mitotic cell

One may notice that a ring of GFP-CaM was clearly visible at the cortical region in the living cell shown in Fig. 3D. A similar structure was found in every mitotic cell expressing the GFP-CaM fusion protein. Fig. 4 are confocal images showing the typical distribution of GFP-CaM in living HeLa cells at different mitotic stages. As one may expect, the distribution of GFP-CaM was dependent on the mitotic stage of the cell. At interphase, the distribution of GFP-CaM protein within the cytoplasm was more or less uniform (see Fig. 3C). When the cells entered metaphase, however, GFP-CaM became concentrated at the polar regions of the mitotic spindle (Fig. 4A). A dense layer of GFP-CaM was also found at the cell cortex underneath the cell membrane (Fig. 4A). This layer of GFP-CaM was relatively thin (approximately 1  $\mu\text{m}$  thick). At anaphase, the cells started to become elongated; the high density GFP-CaM structures migrated with the spindle poles and moved toward the opposite side of the cell. The sub-membrane fraction of CaM was also clearly visible (Fig. 4B). Later, upon the initiation of cytokinesis, a high concentration of GFP-CaM protein appeared to remain at the spindle poles. In addition, fiber-like structures containing high density of GFP-CaM protein were found at the midzone region. Most importantly, high density of GFP-CaM was also found at the newly formed cleavage furrow between the two daughter cells (Fig. 4C). Finally, following the completion of cell division, the

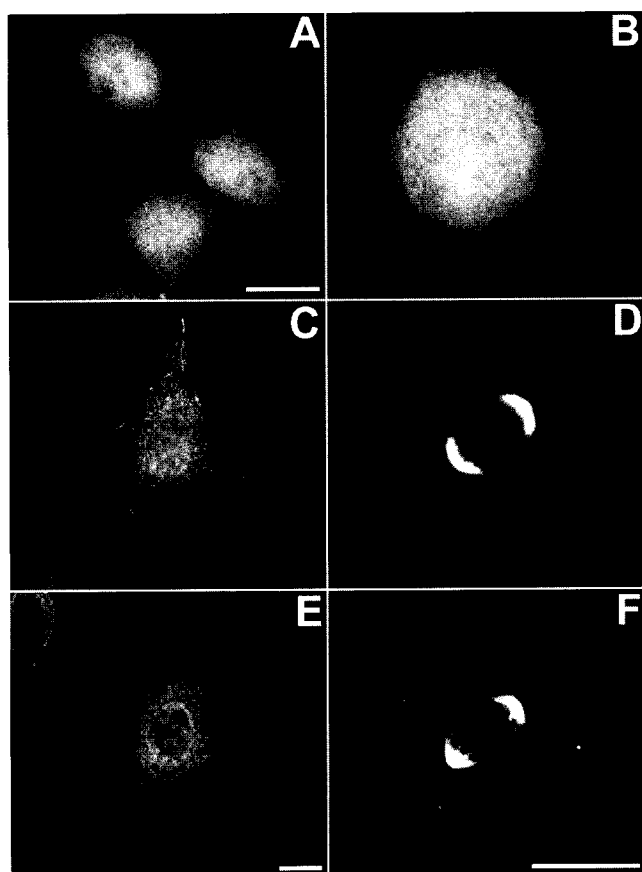


**Fig. 3.** Comparison of the distributions of GFP (A,B), GFP-CaM (C,D), and endogenous CaM (E,F) in interphase cells (A,C,E) or in mitotic cells (B,D,F). (A and B) Fluorescent images of GFP proteins in living HeLa cells. (C and D) Fluorescent images of GFP-CaM proteins in living HeLa cells. (E and F) Fluorescent images of endogenous CaM in fixed HeLa cells as revealed by immunostaining using anti-CaM antibody. Images were recorded using a confocal microscope. Bar, 10  $\mu\text{m}$ .

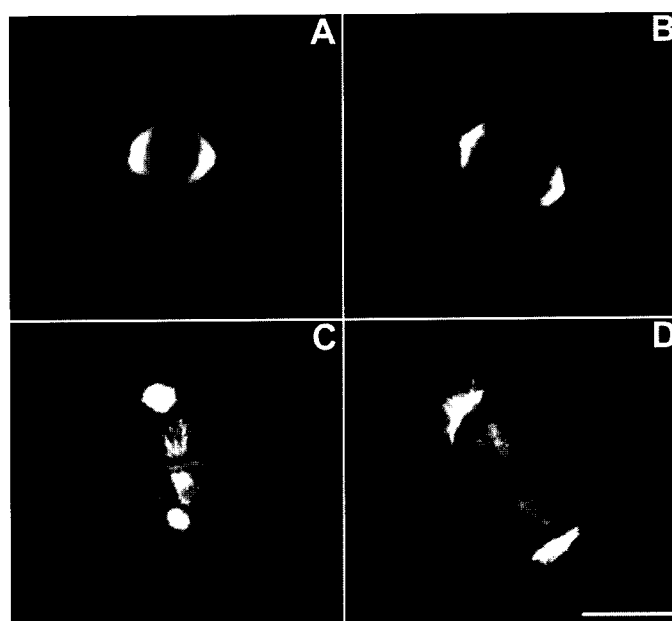


**Fig. 4.** Dynamic redistribution of GFP-CaM protein in living HeLa cells at different mitotic stages. (A) Metaphase; (B) anaphase; (C) telophase; and (D) exit of mitosis. Images were recorded using a confocal microscope. Bar, 10  $\mu\text{m}$ .

two daughter cells became separated. High density of CaM was still observed at the microtubule organizing centers, which were formed from the previous spindle poles. But at the cleavage region, no unusually high density of GFP-CaM was found. Apparently, the aggregation of CaM at the cleavage furrow was a transient phenomenon.

Our finding of the existence of a sub-membrane fraction of CaM in metaphase and anaphase cells was highly interesting. To quantitatively analyze this fraction of CaM, we have conducted a line-scan measurement on mitotic cells that expressed the GFP-CaM gene. The distribution of GFP-CaM (within a single optical section) in an anaphase cell was first measured using a confocal microscope. Then, a line-scan measurement was conducted along the cell equator (see Fig. 5A). The typical result is shown in Fig. 5B. Since the fluorescence intensity is directly proportional to the concentration of GFP-CaM, it is clear that the concentration of GFP-CaM at the cortex region was significantly higher than that in the cytoplasm. Our measurement indicates that, in cells undergoing mitosis, the concentration ratio of GFP-CaM between the cortex and the cytoplasm typically ranged from 1.4- to 2.5-fold (the average ratio was  $1.78 \pm 0.34$ ,  $n=14$ ).

#### A time-dependent measurement of GFP-CaM distribution reveals that a localized elevation of CaM is associated with the cleavage furrow formation

As indicated in Figs 3 and 4, the distribution of GFP-CaM appears to undergo a dynamic change between interphase and the different stages of M-phase. We would like to observe the continuous change of the GFP-CaM distribution in a living cell during this phase transition. When we attempted this measurement using a confocal microscope, we experienced a technical problem. That is, repeated exposure of the cell to laser during sequential confocal measurements often resulted in photo-damaging the cell and caused a stop in the cell division process. To overcome this problem, we used an inverted microscope equipped with a temperature-control stage and a cooled CCD camera to monitor the continuous changes in the distribution pattern of GFP-CaM in a living HeLa cell throughout the entire cell division process. Representative results of this measurement are shown in Fig. 6. In the earlier part of this work, we had observed that the distribution of GFP-CaM in the nucleus depends on the stage of the cell cycle (data not shown). At G<sub>1</sub> phase, very little GFP-CaM was found in the nucleus. GFP-CaM was observed to enter the nucleus in S phase and became highly concentrated in the nucleus in G<sub>2</sub> phase. At the later stage of G<sub>2</sub> phase, GFP-CaM in the nucleus appeared to aggregate into 'lumps' (Fig. 6A). When the cell entered prophase, high densities of GFP-CaM gradually converged at the two sides of the nucleus where the centrosomes are located (Fig. 6B and C). As the mitotic spindle started to form in prometaphase, high densities of GFP-CaM were found in the polar regions of the spindle (Fig. 6D and E). These high densities of GFP-CaM at the spindle poles were maintained through out the metaphase (Fig. 6F), anaphase (Fig. 6G and H), as well as the entire process of cytokinesis (Fig. 6I-P).

Besides the aggregation of GFP-CaM at the polar regions of the spindle, we also observed that an increased amount of GFP-CaM was concentrated at the cell cortex near the cleavage furrow during the onset of cytokinesis (Fig. 6H-L). Later, after the cleavage furrow was clearly established, high densities of

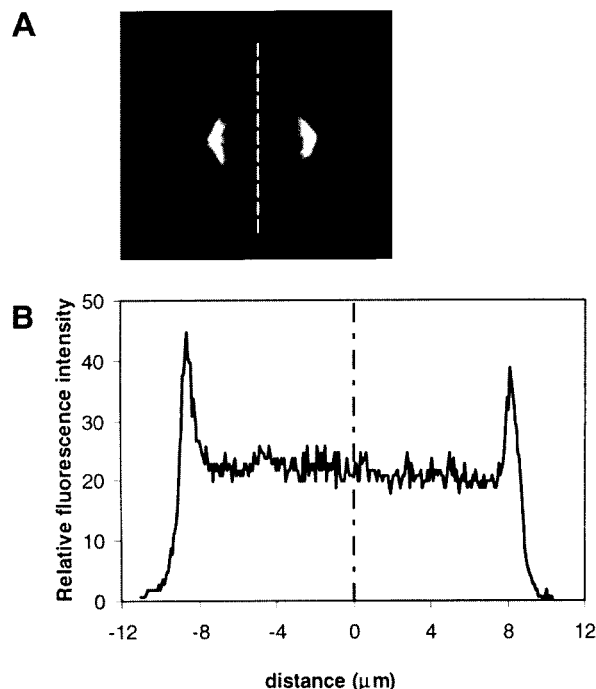


Fig. 5. A line-scan measurement of the distribution of GFP-CaM in a living HeLa cell. (A) The dotted line showing the position of the line-scan measurement. (B) Result of the line-scan measurement. It was evident that, in the anaphase cell, the density of GFP-CaM was higher at the sub-membrane region.

GFP-CaM was also found at the furrow (Fig. 6N-P). These observations are highly interesting and have not been reported before. Since the concentration of the cortex CaM was relatively low and the changes of the cortex GFP-CaM distribution were somewhat subtle, we had repeated this observation in many different HeLa cells and used digital image processing techniques to enhance the images. A typical result of such enhanced measurement is shown in Fig. 7. In late anaphase, before the cytokinesis process started, the concentration of GFP-CaM at the sub-membrane layer was generally low. Yet, a slightly higher concentration of cortical GFP-CaM can be seen at the equator (Fig. 7A). At the beginning of cytokinesis, a cleavage furrow began to appear at the equator of the dividing cell. The density of GFP-CaM was found to elevate at the cell cortex underneath the emerging furrow (Fig. 7B). As the cytokinesis process progressed further, the localized elevation of GFP-CaM at the cleavage furrow region became even more apparent (Fig. 7C and D). This observation suggests that, a localized increase of cortical CaM may be part of the signal transduction mechanisms required for the formation of the contractile ring at the cleavage furrow.

#### Optical measurement using a TA-CaM probe reveals that CaM near the cortex of the cell equator is selectively activated during cytokinesis

To further investigate the functional significance of the sub-membrane fraction of CaM observed in the mitotic cell, we injected an activation probe of CaM into HeLa cells and observed the change of its fluorescence pattern during cell division. TA-calmodulin, i.e. CaM labeled with 2-chloro-

( $\epsilon$ -amino-Lys75)-[6-(4-*N,N*-diethylaminophenyl)-1,3,5-triazin-4-yl], gives a fluorescence intensity 9-fold higher upon binding to  $\text{Ca}^{2+}$  and its target protein (Török and Trentham, 1994; Török and Whitaker, 1994). Thus, TA-CaM can be used as an optical probe to measure the activation of CaM in a specific location of the living cell. This technique has been used in a recent imaging study of calmodulin activation in sea urchin eggs during mitosis (Török et al., 1998). By injecting this TA-CaM probe into HeLa cells, we were able to examine the spatial-specific activation of CaM in the dividing cell. Our experimental results are shown in Fig. 8. When the anaphase cell was about to divide, CaM at the cell cortex near the cell equator was selectively activated (see Fig. 8A). The fraction of CaM accumulated in the spindle poles, on the other hand, was not activated at all. This situation remains unchanged throughout the process of cytokinesis (Fig. 8B-D). That is, only CaM at the cell cortex around the cleavage furrow was found to be activated during cell division. By comparing the results shown in Fig. 8 with those of Fig. 7, one may conclude that, it is the cortical fraction of CaM observed near the cell equator, not the fraction of CaM aggregated at the spindle poles, that seems to be involved in the regulation of cytokinesis.

#### Injection of CaM inhibitor results in suppressing the cytokinesis process

To examine whether CaM is involved in the initiation of the

cytokinesis process, we introduced calmodulin-inhibitory peptides into the mitotic cells by microinjection and studied their effects on cytokinesis. Two types of peptides were injected. The first type, called 'Trp peptide', contains 17 amino acids that mimics the CaM-binding region of myosin light chain kinase (Török and Trentham, 1994). This peptide binds CaM with a very high affinity and prevents CaM from interacting with its target enzymes (Török and Trentham, 1994). The second type of peptide, called 'Tyr peptide', is a point-mutation of the 'Trp peptide', and has a much lower affinity to CaM. It is a far less potent inhibitor.

In order to study the effects of these peptides specifically on cytokinesis, the peptides were injected in a time window between the beginning of anaphase and the initiation of cleavage furrow formation. Table 1 summarizes the results of this injection experiment. In normal cells (i.e. non-injected cells), cleavage furrow was usually formed in about ten minutes after the beginning of anaphase. In cells injected with Trp peptide, 31% of them failed to undergo cell division. For those cells that eventually divided, the time of furrow formation was delayed by more than threefolds. In cells injected with Tyr peptide, all of them went through cytokinesis; the latency before furrow formation, however, was increased about 1.8-fold. These results suggest that activation of CaM is involved in the cleavage furrow formation.

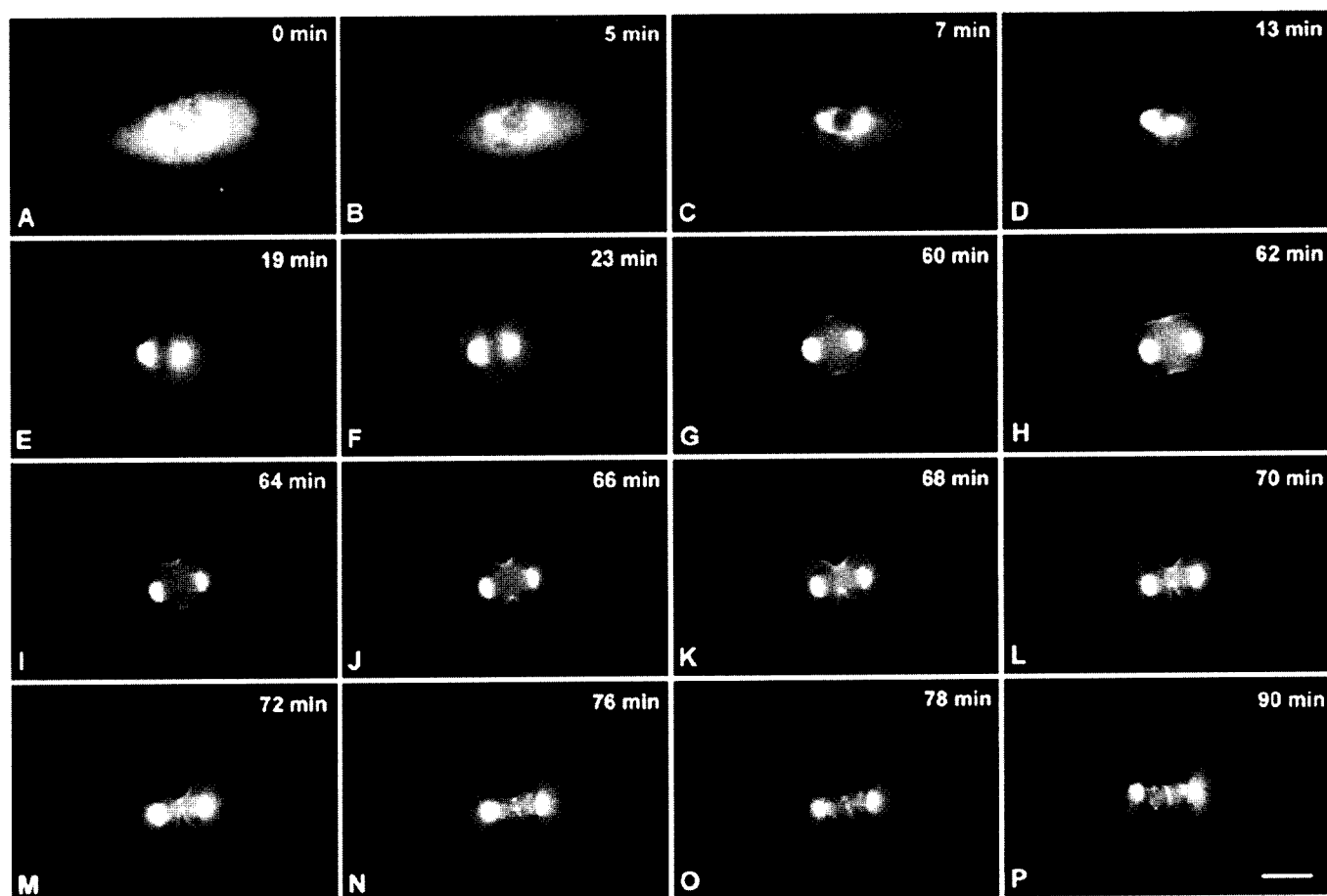


**Fig. 6.** Redistribution of GFP-CaM in a living HeLa cell throughout the entire process of mitosis. The sequence of images shown here started from late G<sub>2</sub> phase. The elapsed time was shown in the upper right hand corner of each panel. The images were recorded using a cooled CCD camera. Bar, 10  $\mu\text{m}$ .

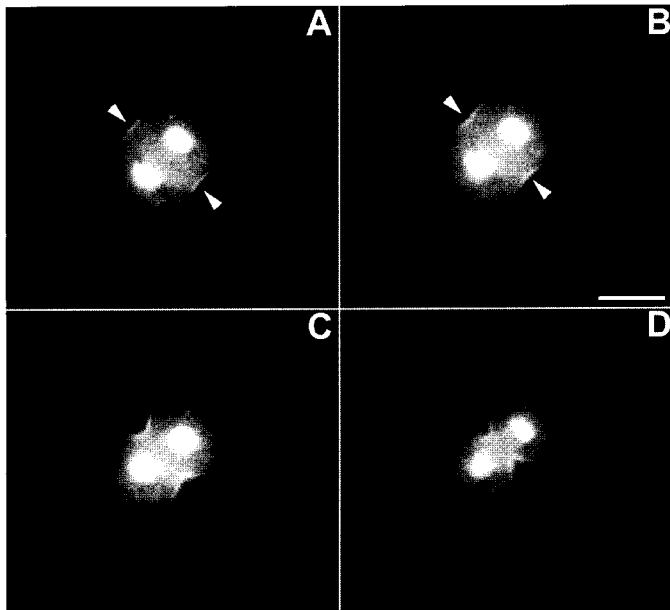


**Fig. 7.** Time-dependent measurement of GFP-CaM distribution in a living HeLa cell undergoing cytokinesis. (A-D) A series of GFP-CaM images obtained at different times (*t*) starting from late anaphase. (A) *t*=0; (B) 2; (C) 6; and (D) 10 minutes. The arrowhead shows the position of the emerging cleavage furrow. Bar, 10  $\mu$ m.

## DISCUSSION

Calmodulin is the major receptor of cytoplasmic  $\text{Ca}^{2+}$  and is known to play an important role in controlling many physiological functions (for reviews see Wang et al., 1985; Means et al., 1991; Takuwa et al., 1995; Niki et al., 1996; Rhoads and Friedberg, 1997). Since involvement of CaM has been implicated in the regulation of cell cycle (Whitaker and Patel, 1990; Rasmussen et al., 1992; Means, 1994; Takuwa et al., 1995), there is a strong interest to investigate the dynamic redistribution of CaM in response to cell division (Zavortink et al., 1983; Hamaguchi et al., 1989; Wilding et al., 1995). The work reported here represents the first detailed examination of the translocation of CaM in mammalian cells using the GFP-fusion gene method. The results of this study have a number of significant implications:

(1) From a technical standpoint, our results clearly demonstrated that the GFP-CaM fusion protein is a highly useful tool for studying the translocation of CaM in living mammalian cells. First, we showed that the functional properties of the GFP-tagged CaM, as determined from our *in vitro* biochemical assays, were very similar to those of the endogenous CaM (see Fig. 2). Second, the distribution of the GFP-CaM fusion protein in the living cell was also found to be consistent with the immunostaining pattern of the endogenous CaM in the fixed cell (see Fig. 3). These results imply that the GFP tagging does not seem to alter the *in vivo* distribution of the CaM molecules in the cell. In addition, our findings also help to clarify a problem on the interpretation of the earlier immunostaining results. Since CaM is a small protein that is at least partly soluble in the cytosol, it could undergo a redistribution during the fixation and Triton treatment used in the immunostaining process (Vos and Hepler, 1998). Recent

**Table 1.** Results of microinjecting calmodulin-inhibitory peptides into early anaphase cells

Treatment	Blockage of furrow formation (%)	Time of furrow formation (minute)*
Control cell	0.0% (0/5)	10.8 $\pm$ 1.3 ( <i>n</i> =5)
Tyr peptide	0.0% (0/24)	18.1 $\pm$ 4.3 ( <i>n</i> =24)
Trp peptide	31.7% (13/41)	35.1 $\pm$ 13.0 ( <i>n</i> =28)

\*Time period between the onset of anaphase and the appearance of cleavage furrow.

studies showed that, when small soluble proteins are introduced into cells, fixation can induce spurious localization of the protein, which may appear to be targeted to the centrosome region of the animal cell (Melan and Sluder, 1992). This finding raised a question on whether the observed CaM aggregation in spindle poles of dividing animal cells as revealed by immunostaining (Welsh et al., 1979) was real or not. This question can now be answered by our GFP-CaM study. Since we showed that, in living cells, part of GFP-CaM was found to aggregate at the polar region of the spindle during cell division, the similar pattern obtained by immunostaining could not be an artifact.

(2) Using this GFP-CaM fusion protein as a probe, we found a high density of CaM was concentrated at the sub-membrane region of the mitotic cell. From earlier immunostaining studies, it was thought that CaM became aggregated only at the polar regions of the spindle in the mitotic cell. Using the GFP-tagging method, we showed that CaM molecules actually aggregated in two separated sub-cellular locations during cell division. Besides the spindle poles, CaM was also concentrated in the sub-membrane region of the mitotic cell. (See Figs 4 and 5). We have investigated that whether these two fractions of localization-specific CaM were bound to different cytoskeleton systems. We found that the sub-membrane fraction of CaM was

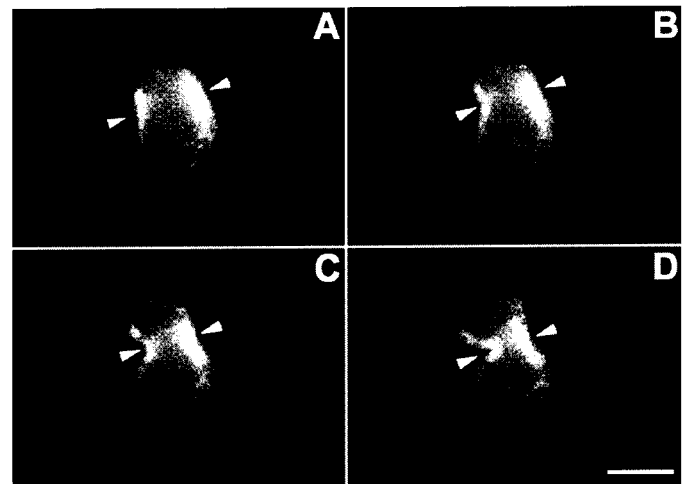


**Fig. 8.** Time-dependent measurement of CaM activation in a living HeLa cell using the TA-CaM probe. The fluorescence image represents mainly the distribution of the activated CaM molecules. (A-D) A series of TA-CaM images obtained at different times (*t*) starting just before the cell undergoing cytokinesis. (A) *t*=0; (B) 2; (C) 6; and (D) 7 minutes. The arrowheads indicate the position where the cleavage furrow emerged. This figure represents typical results obtained from measurements of 18 cells. Bar, 10  $\mu$ m.



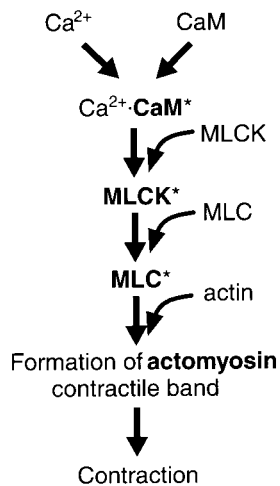


**Fig. 9.** A schematic diagram showing the proposed model of  $\text{Ca}^{2+}$  signaling in its regulation of cytokinesis. The abbreviations are the same as those used in the text: CaM, calmodulin; MLCK, myosin light chain kinase; MLC, myosin light chain. Component written in bold letters and with an asterisk represents the activated form of that component.

co-localized with a cortical network mainly composed of F-actin (unpublished results). The fraction of CaM concentrated at the spindle poles, on the other hand, was shown to bind with microtubules (Deery et al., 1984).

(3) We found evidence suggesting that CaM may play an active role in determining the position (and possibly the timing) of the cleavage furrow formation. Our evidence involves two parts: First, we observed a close spatial and temporal correlation between the aggregation of CaM at the cell equator and the onset of cleavage furrow formation (see Figs 6 and 7). Second, when a highly specific calmodulin-inhibitor, the 'Trp peptide', was injected into HeLa cells in early anaphase (but before cytokinesis), cell cleavage was either blocked or greatly delayed (see Table 1). Injection of a mutated peptide (the 'Tyr peptide') that has a much lower affinity to CaM, on the other hand, did not block cell cleavage and only caused a slight delay. Thus, the blockage (or delay) of cytokinesis was specifically due to the inhibition of CaM. This finding, taken together with the observations of a localized elevation of CaM appearing at the right time and at the right place during cleavage furrow formation, strongly suggests that CaM plays an active role in regulating the initiation of cytokinesis. This interpretation is also consistent with the results of our TA-CaM measurement, which indicate that CaM was selectively activated in the cortical regions around the cell equator during the onset of cytokinesis (see Fig. 8).

This conclusion may fit well with a current hypothesis explaining the molecular mechanism of cleavage furrow formation. In our earlier study using zebrafish embryo as a model system, we found that a localized elevation of free  $\text{Ca}^{2+}$  was closely associated with the initiation of cytokinesis (Chang and Meng, 1995), suggesting the  $\text{Ca}^{2+}$  signal is required for triggering the cleavage furrow formation. To explain how the  $\text{Ca}^{2+}$  signal may regulate the cytokinesis process, we and others have hypothesized that the calcium signal may activate the actomyosin contractile band in the cleavage furrow by a mechanism analogous to that found in smooth muscle (Mabuchi and Takano-

Ohmuro, 1990; Satterwhite and Pollard, 1992; Chang and Meng, 1995). When the  $\text{Ca}^{2+}$  concentration is elevated near the equator, an increased amount of free calcium ions will bind to CaM and activate a CaM-dependent enzyme called 'myosin light chain kinase (MLCK)'. Once activated, MLCK will phosphorylate the Ser-19 site of the light chain of myosin II (MLC) (Satterwhite et al., 1992; Yamakita et al., 1994). Such phosphorylation produces two effects via conformational changes in the myosin molecule: First, it releases the myosin tail from a 'sticky patch' on the myosin head, thereby allowing the myosin II molecules to assemble into short bipolar filaments, which in turn promotes the formation of the contractile band by inducing the aggregation of actin with myosin (Mabuchi and Takano-Ohmuro, 1990). Second, the controlled phosphorylation causes a change in the myosin head and exposes its actin-binding site. This change allows the myosin filaments to interact with the actin filaments and triggers the cleavage furrow contraction.

The down-stream portion of this hypothesis is consistent with findings in recent studies of actin and myosin movement during cytokinesis in both mammalian and *Dictyostelium* cells (Cao and Wang, 1990; Sanger et al., 1994; Moores et al., 1996; Yumura and Uyeda, 1997). The up-stream portion of this hypothesis can be tested by examining the distribution of CaM during cell division. If this hypothetical mechanism is correct, a significant amount of CaM must be available near the cleavage furrow when the contractile band is to be formed during cytokinesis. Results of our GFP-CaM measurements not only indicate that this is indeed the case, but also suggest something that is even more interesting. We observed a localized increase in the concentration of CaM at the cell cortex underneath the cleavage furrow; the timing of this cortical CaM elevation was found to coincide with the onset of cell cleavage (See Fig. 7). These observations suggest that, CaM may be more than a passive component in the  $\text{Ca}^{2+}$  signaling transduction pathway in regulating cell division. Just like  $\text{Ca}^{2+}$  ions, the localized release of which represents an intracellular signal, a localized aggregation of CaM may represent a second signal that is also required for initiating the cytokinesis process. In such a way, the timing and positioning of the cleavage furrow formation can be more precisely controlled. The basic concept of this modified hypothesis is depicted in Fig. 9.

This modified hypothesis may explain a paradox in studying  $\text{Ca}^{2+}$  signaling in cell division. From the results of many studies reported so far, there seems to be a difference in the characteristics of the  $\text{Ca}^{2+}$  signals found in the large embryonic cells and those observed in the smaller cultured mammalian cells. In the embryonic cells, there was clear evidence that a localized elevation of free  $\text{Ca}^{2+}$  concentration ( $[\text{Ca}^{2+}]$ ) is associated with the cleavage furrow formation (Chang and Meng, 1995; Muto et al., 1996; Webb et al., 1997). In the mammalian cultured cells, however, no highly localized elevation of  $[\text{Ca}^{2+}]$  was observed at the cell equator during cytokinesis, only a broadly rising  $[\text{Ca}^{2+}]$  was found to be needed (Tombs and Borisy, 1989). A possible explanation of this difference is that since  $\text{Ca}^{2+}$  is freely diffusible within a local area (between the sources and sinks), it requires a certain amount of space within the cytoplasm to establish a sharp  $\text{Ca}^{2+}$  gradient. And thus, it is more difficult to create a localized  $[\text{Ca}^{2+}]$  change in the small mammalian cells than in the large embryonic cells. But if there is indeed an absence of a steep  $[\text{Ca}^{2+}]$  gradient in the mammalian cell, then what is the signal that determines the

spatial position of the cleavage furrow? The findings in this study may provide the answer to this question. That is, the positioning of the cleavage furrow formation in the mammalian cell may be dependent on the localized aggregation of CaM rather than relying on the spatial pattern of the  $[Ca^{2+}]$  elevation.

During the performance of this work, we became aware of several studies that have overlapping interest with ours. Using the GFP-gene fusion technique, Moser et al. (1997) have studied the distribution of CaM in fission yeast and found that CaM was mainly localized to the spindle pole bodies. They did not mention finding any sub-membrane fraction of CaM. It is highly possible that the distribution of CaM in yeast may be slightly different from that in the mammalian cells, since properties of CaM are known to be different between yeast and vertebrate (Starovasnik et al., 1993). Also, the cytokinesis process is clearly different between fission yeast and animal cells. At present, however, the existence of a sub-membrane fraction of CaM in yeast cannot be entirely ruled out. Due to the small size of the yeast cell, such a fraction of sub-membrane CaM would be very difficult to detect.

In a related study, Vos and Hepler (1998) had examined the distribution of CaM in living plant cell by injecting fluorescently labeled CaM into dividing stamen hair cells of *Tradescantia virginiana*. They found that CaM was uniformly distributed throughout the cell and was not localized with any obvious cellular structure. This result was different from what we observed in HeLa cells using GFP-CaM. Apparently, the distribution of CaM in the dividing plant cells must be significantly different from that in the dividing animal cells. This difference may be related to the fact that the cytokinesis processes are very different between plant and animal cells. For example, the division of cytoplasm in the dividing plant cells is not dependent on the formation of a contractile band.

Török et al. (1998) recently imaged CaM activity in sea urchin eggs undergoing mitosis by using a TA-CaM probe. They found that the spatiotemporal pattern of  $[Ca^{2+}]$  was significantly different from that of the fluorescent image of TA-CaM. This result implies that the activation of CaM may depend on the spatiotemporal distribution of CaM itself. Although their study examined the CaM activation mainly in a time window between NEB (nuclear envelope breakdown) and metaphase/anaphase transition, and thus did not provide any data on cytokinesis, they did mention that 'by anaphase there was a less pronounced but significant activation of calmodulin in the embryo cortex that might be related to cortical contraction and cleavage formation'. This observation is consistent with our findings.

From findings of this work and those of Török et al. (1998), one can see that, in a living cell, the spatiotemporal distribution patterns of  $[Ca^{2+}]$ , CaM and the activation pattern of CaM do not generally coincide with each other. It was particularly gratifying to find that CaM was selectively accumulated and activated at the cell equator during the onset of cytokinesis (see Figs 7 and 8). From our GFP-CaM measurement, we know that a high density of CaM was also localized at the spindle poles. Yet, very little fluorescence signal of TA-CaM was detected in these polar regions (Fig. 8). One interpretation of this observation is that these polar fractions of CaM were not activated during cytokinesis. An alternative interpretation is that these polar fractions of CaM might be bound very tightly to the spindle and thus were not freely exchangeable with the TA-CaM

which was injected into the cell during early metaphase. But even in the second case, there is reason to expect that CaM localized in the spindle poles may not be directly involved in the regulation of cytokinesis. First, it was shown in budding yeast that calmodulin binds to the spindle pole body mainly through the protein Nuf1p/Spc110p; such a binding was known to be  $Ca^{2+}$ -independent (Geiser et al., 1993). Second, there is a significant physical distance between the spindle poles and the cleavage furrow. Third, the aggregation of CaM at the spindle poles was not temporally correlated with the cytokinesis process. Thus, it is unlikely that these polar fractions of CaM are involved in transducing the  $Ca^{2+}$  signal that regulates cytokinesis.

In conclusion, based on results of our imaging measurements using GFP-CaM and TA-CaM probes, and findings from our Trp/Tyr peptide injection experiments, we propose the following model for cytokinesis in mammalian cells: (1) during mitosis, a fraction of CaM is concentrated at the sub-membrane region of the round-up cell (probably through an actin-based transport/anchorage system). (2) Following the metaphase/anaphase transition, this sub-membrane fraction of CaM gradually aggregates underneath the cell equator. (3) At the onset of cytokinesis, the CaM molecules accumulated at the cortex of the cell equator become activated by a broadly rising  $[Ca^{2+}]$ . This localized activation of CaM in turn activates the MLCK, which triggers the formation of the actomyosin contractile band and induces it to contract. There upon, cell cleavage begins to take place.

We are grateful to Drs Wei-min Dai and Minjie Zhang for their help in preparing the TA-CaM probe. We thank Drs Jerry H. C. Wang and Andy Miller for their comments on this manuscript. This work was partially supported by RGC grants HKUST 572/95M and HKUST 6199/97M awarded to D. C. Chang. P. Lu is in a joint training program with the Institute of Biophysics, Chinese Academy of Sciences, Beijing 100101, China.

## REFERENCES

- Berridge, M. J. (1995). Calcium signaling and cell proliferation. *BioEssays* **17**, 491-500.
- Bos-Mikich, A., Whittingham, D. G. and Jones, K. T. (1997). Meiotic and mitotic  $Ca^{2+}$  oscillations affect cell composition in resulting blastocysts. *Dev. Biol.* **182**, 172-179.
- Cao, L. G. and Wang, Y. L. (1990). Mechanism of the formation of contractile ring in dividing cultured animal cells. II. Cortical movement of microinjected actin filaments. *J. Cell Biol.* **111**, 1905-1911.
- Chalfie, M., Tu, Y., Euskirchen, G., Ward, W. W. and Prasher, D. C. (1994). Green fluorescent protein as a marker for gene expression. *Science* **263**, 802-805.
- Chang, D. C., Gao, P. Q. and Maxwell, B. L. (1991). High efficiency gene transfection by electroporation using a radio-frequency electric field. *Biochim. Biophys. Acta* **1992**, 153-160.
- Chang, D. C. and Meng, C. L. (1995). A localized elevation of cytosolic free calcium is associated with cytokinesis in the zebrafish embryo. *J. Cell Biol.* **131**, 1539-1545.
- Chang, D. C. (1997). Experimental strategies in efficient transfection of mammalian cells. *Electroporation. Meth. Mol. Biol.* **62**, 307-318.
- Cubitt, A. B., Heim, R., Adams, S. R., Boyd, A. E., Gross, L. A. and Tsien, R. Y. (1995). Understanding, improving and using green fluorescent proteins. *Trends Biochem. Sci.* **20**, 448-455.
- Deery, W. J., Means, A. R. and Brinkley, B. R. (1984). Calmodulin-microtubule association in cultured mammalian cells. *J. Cell Biol.* **98**, 904-910.
- Finn, B. E. and Forsen, S. (1995). The evolving model of calmodulin structure, function and activation. *Structure* **3**, 7-11.
- Fischer, R., Koller, M., Flura, M., Mathews, S., Strehler-Page, M. A.,

- Krebs, J., Penniston, J. T., Carafoli, E. and Strehler, E. E. (1988). Multiple divergent mRNAs code for a single human calmodulin. *J. Biol. Chem.* **263**, 17055-17062.
- Geiser, J. R., Sundberg, H. A., Chang, B. H., Muller, E. G., Davis, T. N. (1993). The essential mitotic target of calmodulin is the 110-kilodalton component of the spindle pole body in *Saccharomyces cerevisiae*. *Mol. Cell Biol.* **13**, 7913-24.
- Gerdes, H. H. and Kaether, C. (1996). Green fluorescent protein: application in cell biology. *FEBS Lett.* **389**, 44-47.
- Hamaguchi, Y., Iwasa, F., Toriyama, M. and Sakai, H. (1989). A comparative study of the distribution of fluorescently labeled calmodulin and tubulin in the meiotic apparatus of the mouse oocyte. *Cell Struct. Funct.* **14**, 241-248.
- Harlow, E. and Lane, D. (1988). *Antibodies, a Laboratory Manual*. Cold Spring Harbor Laboratory Press, New York.
- Hastings, J. W. (1996). Chemistries and colors of bioluminescent reactions: a review. *Gene* **173**, 5-11.
- Heim, R., Prasher, D. C. and Tsien, R. Y. (1994). Wavelength mutations and posttranslational autooxidation of green fluorescent protein. *Proc. Nat. Acad. Sci. USA* **91**, 12501-12504.
- Heim, R., Cubitt, A. B. and Tsien, R. Y. (1995). Improved green fluorescence. *Nature* **373**, 663-664.
- Heim, R. and Tsien, R. Y. (1996). Engineering green fluorescent protein for improved brightness, longer wavelength and fluorescence resonance energy transfer. *Curr. Biol.* **6**, 178-182.
- Hepler, P. K. (1994). The role of calcium in cell division. *Cell Calcium* **16**, 322-330.
- Kao, J. P. Y., Alderton, J. M., Tsien, R. Y. and Steinhardt, R. A. (1990). Active involvement of  $[Ca^{2+}]_i$  in mitotic process in Swiss 3T3 fibroblast. *J. Cell Biol.* **111**, 183-196.
- Lanzetta, P. A., Alvarez, L. J., Reinach, P. S. and Candia, O. A. (1979). An improved assay for nanomole amounts of inorganic phosphate. *Anal. Biochem.* **100**, 95-97.
- Li, C. J., Wang, B., Wang, J. X., Fan, B. Q. and Zhang, Z. X. (1994). The role of calcium oscillations in mouse oocyte during meiotic maturation. In *Metal Ions in Biology and Medicine*, vol. 3 (ed. Ph. Collery, L. A. Poirier, N. A. Littlefield and J. C. Etienne), pp. 411-415. John Libbey Eurotext, Paris.
- Lu, K. P. and Means, A. R. (1993). Regulation of the cell cycle by calcium and calmodulin. *Endocr. Rev.* **14**, 40-58.
- Mabuchi, I. and Takano-Ohmuro, H. (1990). Effects of inhibitors of myosin light chain kinase and other protein kinases on the first cell division of sea urchin eggs. *Dev. Growth Differ.* **32**, 549-566.
- Means, A. R., VanBerkum, M. F., Bagchi, I., Lu, K. P. and Rasmussen, C. D. (1991). Regulatory functions of calmodulin. *Pharmacol. Therapeut.* **50**, 255-270.
- Means, A. R. (1994). Calcium, calmodulin and cell cycle regulation. *FEBS Lett.* **347**, 1-4.
- Melan, M. A., Sluder, G. (1992). Redistribution and differential extraction of soluble proteins in permeabilized cultured cells. Implications for immunofluorescence microscopy. *J. Cell Sci.* **101**, 731-43.
- Meng, C. L. and Chang, D. C. (1994). Study of calcium signaling in cell cleavage using confocal microscopy. *Biol. Bull.* **187**, 234-235.
- Miyawaki, A., Llopis, J., Heim, R., McCaffery, J. M., Adams, J. A., Ikura, M. and Tsien, R. Y. (1997). Fluorescent indicators for  $Ca^{2+}$  based on green fluorescent protein and calmodulin. *Nature* **388**, 882-887.
- Moores, S. L., Sabry, J. H. and Spudich, J. A. (1996). Myosin dynamics in live *Dictyostelium* cells. *Proc. Nat. Acad. Sci. USA* **93**, 443-446.
- Moser, M. J., Flory, M. R. and Davis, T. N. (1997). CaM localizes to the spindle pole body of *S. pombe* and performs an essential function in chromosome segregation. *J. Cell Sci.* **110**, 1805-1812.
- Muto, A., Kume, S., Inoue, T., Okano, H. and Mikoshiba, K. (1996). Calcium waves along the cleavage furrows in cleavage-stage *Xenopus* embryos and its inhibition by heparin. *J. Cell Biol.* **135**, 181-190.
- Niki, I., Yokokura, H., Sudo, T., Kato, M. and Hidaka, H. (1996).  $Ca^{2+}$  signaling and intracellular  $Ca^{2+}$  binding proteins. *J. Biochem.* **120**, 685-698.
- Poenie, M., Alderton, J. M., Steinhardt, R. A. and Tsien, R. Y. (1986). Calcium rises abruptly and briefly throughout the cell at the onset of anaphase. *Science* **233**, 886-889.
- Prasher, D. C., Eckenrode, V. K., Ward, W. W., Presendergast, F. G. and Cormier, M. J. (1992). Primary structure of the *Aequorea victoria* green-fluorescent protein. *Gene* **111**, 229-233.
- Prasher, D. C. (1995). Using GFP to see the light. *Trends Genet.* **11**, 320-323.
- Rasmussen, C. D., Lu, K. P., Means, R. L. and Means, A. R. (1992). Calmodulin and cell cycle control. *J. Physiol., Paris* **86**, 83-88.
- Ratan, R. R., Maxfield, F. R. and Shelanski, M. L. (1988). Long-lasting and rapid calcium changes during mitosis. *J. Cell Biol.* **107**, 993-999.
- Rhoads, A. R. and Friedberg, F. (1997). Sequence motifs for calmodulin recognition. *FASEB J.* **11**, 331-340.
- Rhyner, J. A., Koller, M., Durussel-Gerber, I., Cox, J. A. and Strehler, E. E. (1992). Characterization of the human calmodulin-like protein expressed in *Escherichia coli*. *Biochemistry* **31**, 12826-12832.
- Sanger, J. M., Dome, J. S., Hock, R. S., Mittal, B. and Sanger, J. W. (1994). Occurrence of fibers and their association with talin in the cleavage furrows of PtK2 cells. *Cell Motil. Cytoskel.* **27**, 26-40.
- Satterwhite, L. L. and Pollard, T. D. (1992). Cytokinesis. *Curr. Opin. Cell Biol.* **4**, 43-52.
- Starovasnik, M. A., Davis, T. N., Klevit, R. E. (1993). Similarities and differences between yeast and vertebrate calmodulin: An examination of the calcium-binding and structural properties of calmodulin from the yeast *Saccharomyces cerevisiae*. *Biochemistry* **32**, 3261-70.
- Takuwa, N., Zhou, W. and Takuwa, Y. (1995). Calcium, calmodulin and cell cycle progression. *Cell Signal.* **7**, 93-104.
- Tombes, R. M. and Borisy, G. G. (1989). Intracellular free calcium and mitosis in mammalian cells: Anaphase onset is calcium modulated, but is not triggered by a brief transient. *J. Cell Biol.* **109**, 627-636.
- Török, K. and Trentham, D. R. (1994). Mechanism of 2-chloro-(epsilon-amino-Lys75)-[6-[4-(N,N-diethylamino)phenyl]-1,3,5-triazin-4-yl]calmodulin interactions with smooth muscle myosin light chain kinase and derived peptides. *Biochemistry* **33**, 12807-12820.
- Török, K. and Whitaker, M. (1994). Taking a long, hard look at calmodulin's warm embrace *BioEssays* **16**, 221-224.
- Török, K., Wilding, M., Groigno, L., Patel, R. and Whitaker, M. (1998). Imaging the spatial dynamics of calmodulin activation during mitosis. *Curr. Biol.* **8**, 692-699.
- Vogel, H. J. (1994). Calmodulin: a versatile calcium mediator protein. *Biochem. Cell Biol.* **72**, 357-376.
- Vos, J. W. and Hepler, P. K. (1998). Calmodulin is uniformly distributed during cell division in living stamen hair cells of *Tradescantia virginiana*. *Protoplasma* **201**, 158-171.
- Wang, J. H., Pallen, C. J., Sharma, R. K., Adachi, A. M. and Adachi, K. (1985). The calmodulin regulatory system. *Curr. Top. Cell. Regul.* **27**, 419-436.
- Waterman-Storer, C. M., Sanger, J. W. and Sanger, J. M. (1993). Dynamics of organelles in the mitotic spindle of living cells: membrane and microtubule interactions. *Cell Motil. Cytoskel.* **26**, 19-39.
- Webb, S. E., Lee, K. W., Karplus, E. and Miller, A. L. (1997). Localized calcium transients accompany furrow positioning, propagation, and deepening during the early cleavage period of zebrafish embryos. *Dev. Biol.* **192**, 78-92.
- Welsh, M. J., Dedman, J. R., Brinkley, B. R. and Means, A. R. (1979). Tubulin and calmodulin. Effect of microtubule and microfilament inhibitors on localization in mitotic apparatus. *J. Cell Biol.* **81**, 624-634.
- Whitaker, M. and Patel, R. (1990). Calcium and cell cycle control. *Development* **108**, 525-542.
- Whitaker, M. (1995). Regulation of the cell division cycle by inositol trisphosphate and the calcium signaling pathway. In *Advances in Second Messenger and Phosphoprotein Research*, vol. 30 (ed. P. Greengard, A. C. Narin and S. Shnollikar), pp. 299-310. Raven Press, New York.
- Wilding, M., Török, K. and Whitaker, M. (1995). Activation-dependent and activation-independent localisation of calmodulin to the mitotic apparatus during the first cell cycle of the *Lytechinus pictus* embryo. *Zygote* **3**, 219-224.
- Yamakita, Y., Yamashiro, S. and Matsumura, F. (1994). In vivo phosphorylation of regulatory light chain of myosin II during mitosis of cultured cells. *J. Cell Biol.* **124**, 129-137.
- Yumura, S. and Uyeda, T. Q. P. (1997). Transport of myosin II to the equatorial region without its own motor activity in mitotic *Dictyostelium* cells. *Mol. Biol. Cell.* **8**, 2089-2099.
- Zavortink, M., Welsh, M. J. and McIntosh, J. R. (1983). The distribution of calmodulin in living mitotic cells. *Exp. Cell Res.* **149**, 375-385.